Macromolecular Research, Vol. 13, No. 2, pp 156-161 (2005)

Thermal Transitions of the Drawn Film of a Nylon 6/Layered Silicate Nanocomposite

Soo-Young Park* and Yang-Hwan Cho

Department of Polymer Science, Kyungpook National University, #1370 Sangyuk-dong, Buk-gu, Daegu 702-701, Korea

Received January 6, 2005; Revised February 15, 2005

Abstract: The thermal transitions of a nylon 6/layered silicate nanocomposite were studied by differential scanning calorimetry and *in-situ* synchrotron X-ray diffraction. The drawn film of the nylon 6/layered silicate nanocomposite typically showed three endotherms in the DSC thermogram; a very broad endotherm at ~120°C (T_1), a double-melting endotherm at ~215°C (T_2), and a high temperature endotherm at ~240°C (T_3). The drawn film of the nylon 6/layered silicate nanocomposite was comprised of a mixture of the α and γ forms, with the α form being generated by drawing the pressed film having the γ form. The melting and crystallization of the crystals were observed at the above thermal transitions during the heating experiment performed at the Pohang X-ray synchrotron radiation source (4C2). The newly generated form was meta-stable and melted at ~T_1. The double-melting at ~T_2 was due to the exothermic crystallization of the α form during the main endothermic melting of the γ form. The α form crystallized at ~T_2 and melted at ~T_3.

Keywords: nylon 6/layered silicate nanocomposite, X-ray, differential scanning calorimetry, synchrotron radiation source, crystal structure.

Introduction

The nylon 6/layered silicate nanocomposite (NCH) has gained a great deal of attention since Toyota researchers first demonstrated a stunning improvement of its mechanical properties, as compared to the pristine nylon 6.[1] Most notable is the unexpected suite of property enhancements obtained from the addition of a few wt% layered silicates, such as the retention of impact strength,[2,3] increased atomic oxygen resistance,[4] and an improved ablative performance.[5] The exfoliation of individual, 1 nm thick aluminosilicate layers in the NCH system was achieved through a high temperature ring-opening polymerization of ε-caprolactams, initiated from aminolauric acid modifiers on the layered silicate surface.[6] From a processing perspective, these NCH systems are very practical, being amenable to injection molding or extrusion.[5,7-11] Substantial fundamental efforts have been devoted to understanding the reinforcing mechanism and impact on the crystal phase development of nylon 6 by the layered silicate. In general, a low volume percent (1-5 vol%) addition of layered silicate impacts polymer crystallite development, having been observed in the vast majority of investigations on semicrystalline polymer nanocomposites. The general effects include induced polymorphism,[12-19] small, irregular crystallites (dendrites, hedrites),[7,14,20,21] an increased crystallization rate,[7,15,16,19,22-25] and alteration of the crystal fraction.[13,26,27] The extent of these effects depends on the process history and specific characteristics of the resin. NCHs have been the most extensively studied semicrystalline nanocomposites to date, greatly facilitated by the substantial investigations available regarding unfilled polymer.

In terms of the crystal structures of nylon 6, Brill[28] and Holmes *et al.*[29] determined the α-form in the fiber specimen. This form consists of a monoclinic unit cell (a=9.56 Å, b=17.24 Å, c=8.01 Å, β=67.5°) with the b dimension being along the fiber axis. There are eight monomeric units in the unit cell with an extended-chain sheet structure and hydrogen bonding between the anti-parallel chains.[30] Such an arrangement can be achieved by adjacent re-entry of the folded chains, as in quiescent crystallization. Homes *et al.*[29] and Arimoto *et al.*[31] also determined the γ form of nylon 6, consisting of a monoclinic unit cell (a=9.33 Å, b=16.88 Å, c=4.781 Å, β=121°) with the b dimension being along the fiber axis.[30] This form has four monomeric units in the unit cell and hydrogen bonding between the parallel chains.[30] The important feature of nylons is that the structure undergoes a crystalline transition which has been well documented and is known as the Brill transition.[32] In nylon-6,6, the RT α-phase transforms into a pseudohexagonal struc-

*e-mail: psy@knu.ac.kr

ture by heating.[32] A crystalline transition is also reported for nylons-4,6,[33] -6,10,[33] and -6,12.[33,34] Murthy *et al.*[35] have observed that the room temperature monoclinic structure of nylon 6 transforms into a high temperature monoclinic structure due to heating from RT and it was considered it to be a Brill transition. However, it is uncommon to observe the Brill transition in nylon 6. The double-melting peaks have been observed for some nylon 6[36,37] and some NCH systems.[38,39] There are, however, contradictory explanations regarding the nature of such melting peaks. First, some researchers suggest that the double-melting peaks are due to the mixed α- and γ-phases of nylon 6 with the lower temperature peak corresponding the melting temperature of the γ-phase.[38,39] Second, some studies show that the double-melting peaks are due to melting/ recrystallization/ re-melting of the nylon 6 while the intermediate structure between the crystalline and amorphous phases was suggested for the structure produced during recrystallization. Third, the population of two distinct sized crystals causes the double-melting.[40]

The objective of this study is to explore thermal transitions of the NCH system with biaxially protruded and zone-drawn films. We recently studied the three-dimensional structure of the zone-drawn film of the NCH.[41] The quenched biaxially protruded films exhibited a uni-planar crystalline texture with the *b*-axis of the dominant γ form oriented towards the normal to the film surface, and the surface of the layered silicate was oriented parallel to the film surface. The α crystallites were developed upon uniaxial drawing. The newly formed α exhibited a uniaxial texture, whereas the γ form exhibited a three-dimensional texture with the *a*-axis (or *c*-axis) normal to the film surface and the *b*-axis parallel to the drawing direction. In this study, *in-situ* wide angle X-ray scattering experiments were performed with an X-ray beam in the three principal directions exposed on the zone-drawn film, in order to elucidate the mechanism responsible for the several endothermic peaks observed in the DSC measurement.

Experimental

Materials and Film Drawing. Commercially available 5 wt% (NCH5) nylon 6/layered silicate *in-situ* polymerized polymer/layered silicate nanocomposite (PLSN) materials were obtained from Ube Industries, Ltd (Japan).[42] Ring-opening polymerization of ε-caprolactam initiated by pendant carboxylic acids on the surface of the modified montmorillonite reportedly resulted in approximately 50% of the nylon 6 chains tethered to the surface of the montmorillonite *via* ionic interaction of the primary ammonium cation.[43] The PLSNs were obtained as extruded pellets and dried under a vacuum at 70~80 °C for 12 hrs prior to compression into the ~100 μm film under a pressure of 3,000 psi. Zone drawing was carried out at ~210 °C by moving a pair of narrow-band heaters [70 mm × 5 mm × 0.5 mm (length × width × thickness)] along the film. A compressed film was drawn under tensions controlled by different dead weights on an Instron. The heat band speed was 10 mm/min. The final drawing ratio controlled by the weights was up to × 4. The decrease in thickness was approximately in proportional to the increase in length.

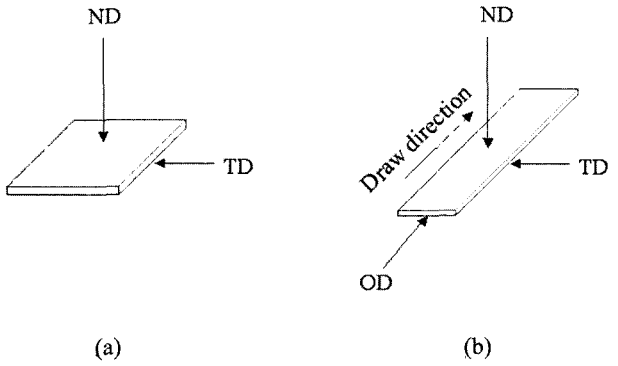

Figure 1. The directions of X-ray beams for structural analysis of (a) the biaxially protruded and (b) the drawn films. Normal Direction, ND: normal to film surface; Transverse Direction, TD: perpendicular to normal (and drawing) direction; Orthogonal Direction, OD: parallel to the drawing direction.

X-ray Characterization. Film specimens for the three dimensional X-ray analysis were prepared by stacking the ~1.5 mm wide films such that the x-ray specimen was ~1 mm in thickness. Figure 1 summarizes the interrelation between the drawing direction and scattering experiment. Synchrotron WAXS measurements were performed on Beamline 4C2 at Pohang Light Source (Korea) where a W/B4C double multilayer monochromator delivered monochromatic X-rays with a wavelength (λ) of 0.1542 nm and a resolution of $\Delta\lambda/\lambda$=0.01. A flat Au mirror was used to reject the higher harmonics from the beam. A 2-D CCD camera (Princeton Instruments Inc., SCX-TE/CCD-1242) was used to collect the scattered X-rays. The heating experiment was performed using the Metler hot stage. The sample thickness was ~1 mm, and the exposure time was ~1 min. The two-dimensional X-ray patterns were integrated along the azimuthal direction to provide one-dimensional curves at each temperature.

Thermal Properties. DSC experiments were carried out in a Dupont 2000 Thermal Analyzer. The temperature and heat flow scales were calibrated using standard materials. The sample weight used was ~6 mg.

Results and Discussion

Figure 2 shows the DSC thermograms of the NCH film drawn at different drawing ratios. A broad endotherm at ~120 °C (T_1), a double-melting peak at ~215 °C (T_2) and a small endotherm at ~240 °C (T_3) were typically observed

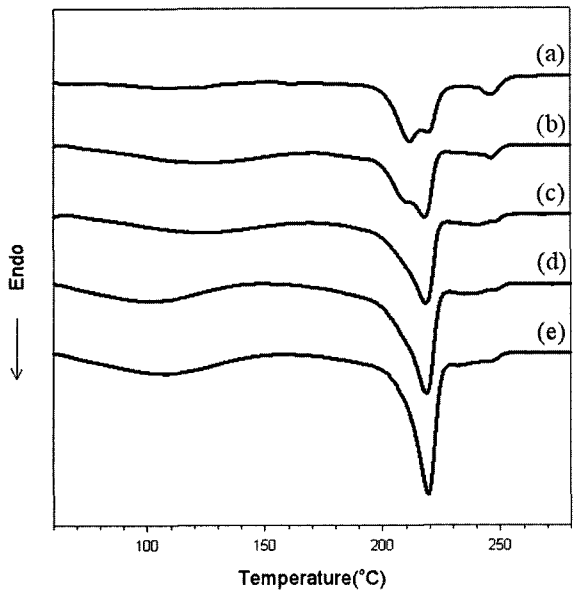

Figure 2. DSC thermograms of the NCH film drawn at the drawing ratios of (a) × 1 (the pressed film), (b) × 1.5, (c) × 2.0, (d) × 2.5, and (e) × 3.0 measured at 10°C/min.

although transition temperatures changed a little bit from sample-to-sample. The broad endotherm at T_1 was barely observed for the pressed film and its enthalpy increased with the increase of the drawing ratios. The double-melting behavior at T_2 was observed for the pressed film. The valley of the double-melting peak decreased with the increase of the drawing ratio, and finally changed into the single-melting peak for the highly drawn film. The high temperature endotherm at T_3 was broad over the range between 230 and 250 °C with a clear transition at ~250 °C. The DSC thermogram for the drawn film of the pure nylon 6 made by the same method showed only one endotherm at T_2.

Figure 3(a) shows the DSC thermograms of the pressed NCH films with different heating ratios. The shape of the double-melting peak at T_2 was dependent upon the heating rate. The valley of the double-melting shifted to the higher temperature with the increase in the heating rate. The endotherm at T_3 did not change with the heating rate. Figure 3(b) shows the DSC thermograms of the drawn films at × 3.0 with different heating ratios. The transition at T_1 was strongly dependent on the heating rate and the maximum increased with the heating rate, indicating that the structure developed during the drawing was meta-stable and melted at the relatively low temperature, T_1.

Figure 4 shows the wide angle X-ray pattern of the pressed film with an X-ray beam along the ND and TD directions. The strong reflection at 2θ=~21°(d=~4.2 Å) in both the ND and TD patterns was the $\bar{2}01/200/001$ reflection of the γ form. The *020* reflection (2θ=10.6°(d=8.37 Å)) of the γ form of the TD pattern is stronger than that of the ND one due to the uni-planar orientation. The shoulder reflection at

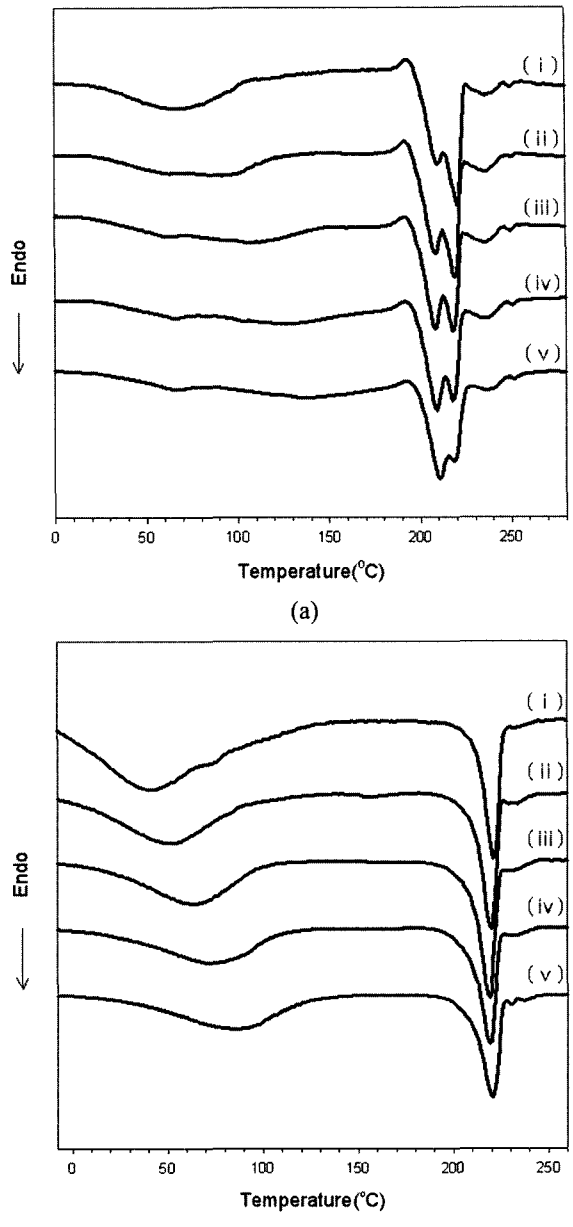

Figure 3. DSC thermograms of (a) the pressed and (b) the three times drawn NCH films with different heating ratios of (i) 2 °C/min, (ii) 5 °C/min, (iii) 10 °C/min, (iv) 20 °C/min, and (v) 40 °C/min.

2θ = ~20° in the TD pattern is the clay's *020/110* reflection.[44] This reflection did not vanish until 280 °C which was far above the melting temperature of the nylon crystal. It is evident from the X-ray pattern that most of the crystal part of the pressed film was the γ form. The strong $\bar{2}01/200/001$ reflection did not change very much until the crystal melted. The double-melting peak was observed for the pressed film in the DSC thermogram. The claim that the double-melting peak corresponds to the α and γ phases of nylon 6, with the

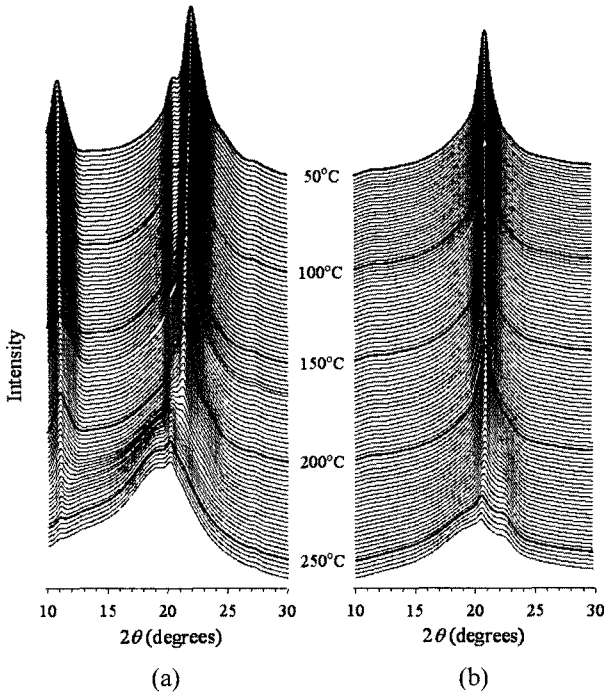

Figure 4. *In-situ* wide angle X-ray patterns of the pressed film with X-ray beam along the (a) TD and (b) ND directions during heating.

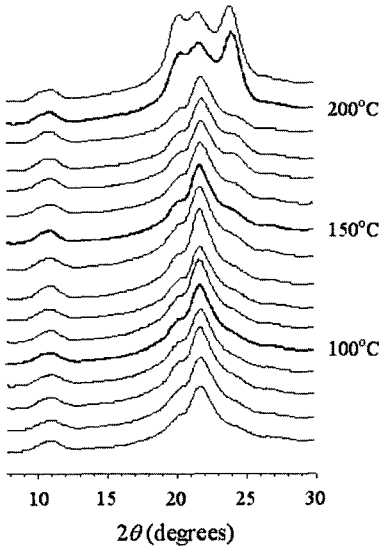

Figure 5. Wide angle X-ray patterns of the pressed film with X-ray beam along the ND direction after annealing at different temperatures during 2 hrs.

lower temperature for the γ phase and the higher one for the α phase, does not seem to be right in this case. A broad additional peak at $2\theta = \sim 23°$, however, appeared at $\sim T_2$. The broadness of this reflection indicates that the developed crystalline structure is quite small and disordered. The position of this reflection is similar to that of the *002* reflection of the α form. Figure 5 shows the wide angle X-ray ND pattern of the pressed film annealed at different temperatures for 2 hrs. Until 190 °C, the X-ray patterns were similar to those before annealing, indicating that the γ form was dominated. The X-ray patterns, however, of the films annealed at 200 and 210 °C show that the *200* and *002* reflections of the α form were developed. The film could not be annealed above 210 °C due to its melting. The temperatures of 200 and 210 °C coincide with that at which the additional reflection appeared in Figure 4. Thus, the newly developed reflection, during the heating of the pressed film, was the *002* reflection of the α form, which is the strongest reflection in the α form. These results strongly suggest that the origin of the double-melting peaks is the recrystallization of the α form with the simultaneous melting of the main γ form. The small exotherm peak during crystallization would make the valley in the main melting endotherm.

Figure 6 shows the wide angle X-ray patterns of the drawn film with X-ray beam along the ND, TD, and OD directions. The *200* and *002* reflections of the α phase at d=4.52 Å and d=3.79 Å are observed in the ND, TD and OD patterns and straddle the $\bar{2}01/200/001$ reflections of the γ phase. The *020* reflection of the TD pattern is stronger than that of the ND pattern and is similar to the protruded film, indicating that the planar orientation obtained during the pressing of the film was maintained after the film drawing. The presence of the *200* and *002* reflections of the α phase indicates that the α phase was produced during the drawing process, as commonly reported for the drawing of the γ-containing nylon 6 fibers.[29,45,46] The OD pattern (Figure 6(c)) shows the *h0l* reflections as well as the absence of the *020* reflection of the γ phase, implying that the chain axis within the γ-crystallites is parallel to the drawing direction (note that the *b* axis is the chain axis). The intensity of the *200* and *002* reflections of the α form decreased gradually with the increase of the temperature and finally disappeared at 190 °C. The 2θ position of the *200* reflection increased and that of the *002* reflection decreased with the increase of the temperature, which is similar to the Brill transition. The decrease of the gap of the 2θ position of these two reflections along with the increase of the temperature indicates that the chain-chain spacing increases with the increased temperature, and the sheet-sheep distance decreases. The decrease of the intensity of the *200* and *002* reflections of the α phase does not incorporate the increase of the other reflections, indicating that the α-phase was not transformed by a transition but melted during heating unlike the Brill transition. The decrease of the intensity of the *200* and *002* reflections of the α form is in agreement with the T_1 transition in the DSC experiment, suggesting that the origin of the broad endotherm was the melting of the α phase. This explanation manifests the absence of the broad endotherm for the pressed film, which has the dominated γ-phase. The

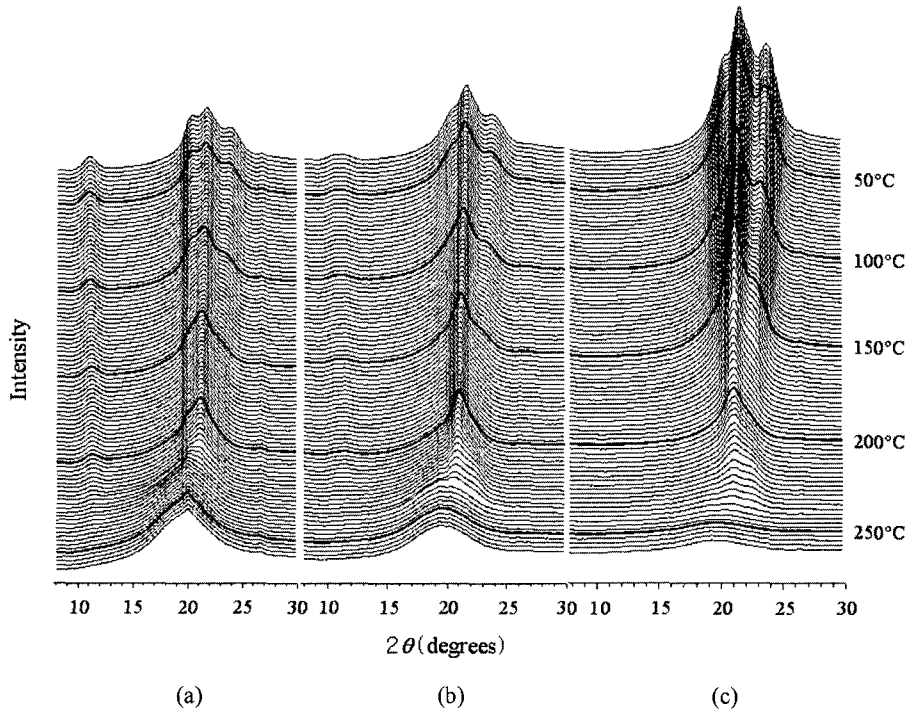

Figure 6. Wide angle X-ray patterns of the drawn film with X-ray beam along the (a) ND, (b) TD, and (c) OD directions.

new reflection was also developed at a temperature higher than 200 °C, which is similar to that of the pressed film, indicating that the α form was developed during the melting of the γ form. The newly developed α form was able to withstand the melting of the γ form in both the pressed and drawn films. In the DSC thermogram, the additional broad endotherm was found after melting, although the shape of the endotherm is quite complex. This broad endotherm, however, is related to the melting of the newly formed α form although the study on the detail structural change needs more resolution in the X-ray pattern.

Conclusions

In this article, we have investigated the thermal transitions of the drawn film of the nylon 6/layered silicate nanocomposite. The wide X-ray diffraction showed that the α form was developed during drawing the pressed film, which mainly consisted of the γ form. The drawn film of the NCH showed the three endotherms in the DSC thermogram: the very broad endotherm at ~120 °C (T_1), the double-melting at ~215 °C (T_2), and the high temperature endotherm at ~240 °C (T_3). The *in-situ* wide angle X-ray patterns were gathered during heating experiment at Pohang synchrotron radiation source to elucidate the structural changes at each transition. The synchrotron data showed that the newly generated α form was meta-stable and melted at ~T_1, the double-melting at ~T_2 was due to the exothermic crystallization of the α form during the main endothermic melting of the γ form, and the α form crystallized at ~T_2 melted at ~T_3. We also found that the newly developed α crystal, which was mechanically induced by drawing, differs from the high temperature α form, which was thermally induced. The former one was meta-stable with low melting temperature although the later one was stable with high melting temperature.

Acknowldgements. This work was supported by a Grant from the Korean Research Foundation (KRF-KRF-2004-002-D00123) and Brain 21 program. And this work was supported in part by the Ministry of Science & Technology (MOST), POSCO, the Center for Integrated Molecular System (Korea Science & Engineering Foundation) and the KISTEP (Basic Research Grant of Nuclear Energy, MOST).

References

(1) A. Okada and A. Usuki, *Polym. Prepr. (Am. Chem. Sco., Div. Polym. Chem.)*, **28**, 447 (1987).
(2) Kojima, Y. Usuki, A. Kawasumi, M. Okada, O. Fukushima, Y. Kurachi, and T. Kamigaito, O. *J. Mater. Res.*, **8**, 1185 (1993).
(3) L. Liu, Z. Qi, and X. Zhu, *J. Appl. Polym. Sci.*, **71**, 1133 (1999).
(4) D. T. Hseih, T. B. Lloyd, and S. K. Rutledge, *Int. SAMPE Symp. Proc., Conf. Proc. of 1998 Meeting (Part 2 of 2)*, **43**, 1170 (1998).
(5) R. A. Vaia, G. Price, P. N. Ruth, H. T. Nguyen, and Lichtenhan. *J. Appl. Clay Sci.*, **15**, 67 (1999).
(6) A. Okada, M. Kawasumi, A. Usuki, Y. Kojima, T. Kurauchi,

and O. Kamigaito, *Mater. Res. Soc. Symp. Proc.*, **171**, 45 (1990).
(7) Y. Ke, C. Long, and Z. Qi, *J. Appl. Polym. Sci.*, **71**, 1139 (1999).
(8) Y. Kojima, A. Okada, M. Kawasumi, A. Okada, Y. Fukushima, T. Kurauchi, and O. Kamigaito, *J. Mater. Res.*, **8**, 1185 (1993).
(9) P. B. Messersmith and E. P. Giannelis, *J. Polym. Sci.; Part A: Polym. Chem.*, **33**, 1047 (1995).
(10) Y. Kojima, A. Usuki, M. Kawasumi, A. Okada, T. Kurauchi, and O. Kamigaito, *J. Appl. Polym. Sci.*, **49**, 1259 (1993).
(11) R. Krishnamoorti and E. P. Giannelis, *Macromolecules*, **30**, 4097 (1997).
(12) P. Maiti, P. H. Nam, M. Okamoto, and T. Kotaka, *Polym. Eng. Sci.*, **42**, 1864 (2002).
(13) C. R. Tseng, S. C. Wu, J. J. Wu, and F. C Chang, *J. Appl. Polym. Sci.*, **86**, 2492 (2002).
(14) K. Strawhecker and E. Manias, *Chem. Mater.*, **12**, 2943 (2000).
(15) [a] B. Han, G. Ji, S. Wu, and J. Shen, *Eur. Polym. J.*, **39**, 1641 (2003); [b] Z. Z. Yu, M. Yang, Q. Zhang, C. Zhao, and Y. W. Mai, *J. Polym. Sci.; Part B: Polym. Phys.*, **41**, 1234 (2003); [c] X. Liu, Q. Wu, and L. A. Berglund, *Polymer*, **43**, 4967 (2002).
(16) [a] Z. Liu, P. Zhou, and D. Yan, *J. Appl. Polym. Sci.*, **91**, 1834 (2004); [b] G. Zhang and D. Yan, *J. Appl. Polym. Sci.*, **88**, 2181 (2003); [c] L. Y. Wang, S. Q. He, L. C. Hao, C. S. Zhu, and Z. N. Qi, *Gaofenzi Cailiao Kexue Yu Gongcheng*, **18**, 62 (2002).
(17) D. M. Lincoln, R. A. Vaia, Z. G. Wang, B. S. Hsiao, and R. Krishnamoorti, *Polymer*, **42**, 9975 (2001).
(18) X. Liu, Q. Wu, L. A. Berglund, and Z. Qi, *Macromol. Mater. Eng.*, **287**, 515 (2002).
(19) T. M. Wu, E. C. Chen, and C. S. Liao, *Polym. Eng. Sci.*, **42**, 1141 (2002).
(20) P. H. Nam, P. Maiti, M. Okamoto, T. Kotaka, N. Hasegawa, and A. Usuki, *Polymer*, **42**, 9633 (2001).
(21) E. Devaux, S. Bourbigot, and A. E. Achari, *J. Appl. Polym. Sci.*, **86**, 2416 (2002).
(22) V. Krikorian, M. Kurian, M. E. Galvin, A. P. Nowak, T. J. Deming, and D. J. Pochan, *J. Polym. Sci.; Part B: Polym. Phys.*, **40**, 2579 (2002).
(23) C. M. Carter, *Annu. Tech. Conf.-Soc. Plast. Eng.*, **3**, 3210 (2001).
(24) T. M. Wu and J. Y. Wu, *J. Macromol. Sci. Phys.*, **41**, 17 (2002).
(25) T. D. Fornes and D. R. Paul, *Polymer*, **44**, 3945 (2003).
(26) H. D. Wu, C. R. Tseng, and F. C. Chang, *Macromolecules*, **34**, 2992 (2001).
(27) Q. Wu, X. Liu, and L. A. Berglund, *Macromol. Rapid Commun.*, **22**, 1438 (2001).
(28) R. Brill, *Z Physik Chem. B*, **53**, 61 (1943).
(29) R. Holmes, D. W. Bunn, and D. L. Smith, *J. Polym. Sci.*, **17**, 619 (1955).
(30) J. Francisco, R. Medellin, C. Burger, B. S. Hsiao, B. Chu, R. A. Vaia, and S. Phillips, *Polymer*, **42**, 9015 (2001).
(31) H. Arimoto, M. Ishibashi, M. Hirai, and Y. Chatani, *J. Polym. Sci.*, **3**, 317 (1965).
(32) R. Brill, *J. Prakt. Chem.*, **161**, 49 (1942).
(33) C. Ramesh, *Macromolecules*, **32**, 3721 (1999).
(34) H. J. Biangardi, *J. Macromol. Sci., Phys. B*, **29**, 139 (1990).
(35) N. S. Murthy, S. A. Curran, S. M. Aharoni, and H. Minor, *Macromolecules*, **24**, 3215 (1991).
(36) M. Todoki and T. Kawaguchi, *J. Polym. Sci.; Part B: Polym. Phys.*, **15**, 1067 (1977).
(37) T. Itoh, H. Miyaji, and K. Asai, *Jap. J. Appl. Phys.*, **14**, 206 (1975).
(38) L. Liu, X. Zhu, and Z. Qi, *Gaofenzi Xuebao*, **3**, 274 (1999).
(39) T. Wu and C. Liao, *Macromol. Chem. Phys.*, **201**, 2820 (2000).
(40) Z. Ergungor, M. Cakmak, and C. Batur, *Macromol. Symp.*, **185**, 259 (2002).
(41) S. Y. Park, Y. H. Cho, and R. A. Vaia, *Macromolecules*, **38**, 1729 (2005).
(42) Y. Kojima, T. Matsuoka, H. Takahashi, and T. Kurauchi, *J. Appl. Polym. Sci.*, **51**, 683 (1994).
(43) A. Usuki, Y. Kojima, M. Kawasumi, A. Okada, Y. Kukushima, T. Kurauchi, and O. Kamigaito, *J. Mater. Res.*, **8**, 1179 (1993).
(44) J. Francisco, R. Medellin, B. S. Hsiao, B. Chu, and B. X. Fu, *J. Macromol. Sci.; Part B: Physics*, **42**, 201 (2003).
(45) H. Arimoto, *Kobunshi Kagaku*, **19**, 212 (1962).
(46) K. Miyasaka and K. Ishikawa, *J. Polym. Sci.; Part A: Polym. Chem.*, **6**, 1317 (1968).